Journal of Applied Electrochemistry **30**: 831–838, 2000.

Some aspects of removal of copper and cobalt from mixed ion dilute solutions

A.S. PILLA[1], M.M.E. DUARTE[1,2]* and C.E. MAYER[1,2]
[1]*Instituto de Ingeniería Electroquímica y Corrosión, Universidad Nacional del Sur, 8000 Bahía Blanca, Argentina*
[2]*Comisión de Investigaciones Científicas de la Provincia de Buenos Aires*
*(*author for correspondence, fax: +54 291 4595182, e-mail: mduarte@criba.edu.ar)*

Received 30 November 1998; accepted in revised form 8 November 1999

Key words: anodic linear sweep voltammetry, cobalt, copper, electrodeposition, vitreous carbon

Abstract

Some aspects of the electrodeposition of copper and cobalt from aqueous sulphate solutions containing low concentrations of their ions were studied with a view to heavy metal removal via an electrochemical process. Both metals were deposited on a vitreous carbon rotating disc electrode. Deposits formed under different conditions were studied employing linear sweep voltammetry, scanning electron microscopy and EDAX surface analysis. Constant potential electrolysis was used to simulate recovery in a laboratory batch reactor. Copper can be deposited without cobalt interference at potentials as cathodic as −1.0 V despite high Co concentrations. At more negative potentials, both metals are deposited simultaneously, although the copper proportion in the binary mixture is greater than that corresponding to the solution concentration ratio. Voltammetry studies effected under conditions in which codeposition occurs show only minor changes in copper behaviour. On the other hand, cobalt behaviour exhibits significant modifications. Even though formation of an intermetallic compound is possible, ASVL and microscopy tests indicate cobalt deposition in different crystalline forms as the more probable cause. In turn, cobalt deposition depends on the polarization conditions of the electrode and on the cobalt and copper concentrations.

1. Introduction

Electrodeposition of metals, particularly from aqueous solutions, is an attractive method for the recovery of metal ions from different industrial effluents such as plating, metal finishing and electronics [1, 2]. In many cases, these ions represent an environmental hazard and legislation generally imposes maximum discharge levels regarding quantity and concentration. In the present work, the electrodeposition of copper and cobalt from solutions containing their ions in low concentration is studied. This type of effluent can originate in wash wastewater arising from the fabrication of printed circuits or thin films for magnetic recording devices, in which both metals are deposited by electroless plating or electrodeposition.

Copper recovery has been widely used as test reaction [3–9], but cobalt recovery has drawn less interest [10–12]. On the other hand references may be found to the simultaneous deposition of Cu/Ni [13, 14], Cu/Cd [15, 16], Cu/Pb [13], Co/Zn [17], Co/Ni [18] etc., but information on the basic aspects of the electrochemistry of the system Cu/Co is scarce [19, 20]. The equilibrium phase diagram of the latter system shows little mutual solubility of Co and Cu below 500 °C and alloys cannot be obtained by conventional methods. However, electrodeposition of Cu–Co multilayers has attracted interest in recent years since they present unusual magnetic properties [21–28]. Most electrodeposition studies have been primarily concerned with the attainment of a particular deposit morphology and relating it to the plating conditions. These studies, although important for the development of plating, have not been focused on the elucidation of the kinetics or mechanism of electrodeposition reactions, especially electrodeposition of alloys.

This work examines some aspects of the electrodeposition of both metals from sulphate solutions containing low concentrations of both ions. Initially, deposits formed under different conditions were studied employing linear sweep voltammetry, scanning electron microscopy and EDAX surface analysis to evaluate the composition and electrochemical behaviour of the binary mixtures. Thereafter, simulating an industrial treatment, a batch reactor with a reticulated vitreous carbon rotating cylinder cathode was operated at constant potential conditions over a prolonged time to determine current efficiency and conversion for both metals.

2. Experimental details

Electrochemical experiments were carried out in a conventional glass cell with a 350 cm^3 solution volume. A vitreous carbon (The Electrosynthesis Co.) rotating

disc ($d = 0.3$ cm) was used as a working electrode for the first tests. The experimental arrangement included a platinum plate counter electrode, which was separated from the principal compartment by a porous glass diaphragm, and a saturated calomel reference electrode that was located in a Luggin capillary. All the potentials mentioned in this work are referred to the saturated calomel electrode (SCE). Before electrolysis the vitreous carbon disc was polished with emery paper (grit 1200) and washed with distilled water.

In voltammetric experiments, the working electrode rotation speeds were modified from 50 to 900 rpm and potential was controlled by means of a Wenking LB75L potentiostat. The electrochemical circuit was completed with a LYP wave generator and an X–Y Hewlett Packard 7004B recorder.

The test electrolytes were aqueous solutions of 0.5 M $Na_2SO_4 + x\,CuSO_4 + y\,CoSO_4$ (pH 2), where x and y were varied between 10 and 500 ppm. The electrolyte was deaerated by nitrogen bubbling.

In the simulated recovery experiments, a similar arrangement to that described was employed, but using a reticulated vitreous carbon (RVC) rotating cylinder as working electrode; this had the following characteristics: 0.5 cm diameter, 1.0 cm height, porosity 80 ppi (pores per inch). A constant rotation speed of 500 rpm was used. The working electrode was held at constant potential using a Wenking HP88 potentiostat connected to an analogic digital interface and commanded by a personal computer.

Concentrations of the metal ions were analysed using a 20D Spectronic spectrophotometer. The bicinchoninate method for measuring copper was chosen due to the ease of analysis, high sensitivity and freedom of interference [29]. For cobalt, the P.A.N. (1-(2-pyridylazo)-2-naphtol) procedure was selected [29]. Both methods were checked against plasma emission spectroscopy (Shimadzu ICPS 1000 III). The surface studies were effected with a scanning electronic microscope Jeol 100, equipped with an EDAX microanalysis system.

3. Results and discussion

3.1. *Copper electrodeposition*

Figure 1 shows polarization curves corresponding to copper electrodeposition on a vitreous carbon rotating disc electrode for several rotation speeds. The reaction occurs in the potential range from 0 to −0.6 V without hydrogen evolution, showing the limiting current plateau indicative of a mass transfer controlled process.

According to the Levich equation [30], the system shows a linear relationship between the limiting current and $\omega^{1/2}$. This behaviour is characteristic of mass transport control. The diffusion coefficient for copper ions was calculated from the slope using the Koutecky–Levich equation for mixed control [31]. An average diffusion coefficient of 5.3×10^{-6} cm^2 s^{-1} was estimated from the values obtained at different concentrations. This coefficient is lower than values generally reported for copper ion [31–33], although it is similar to that determined using a similar technique and conditions [34].

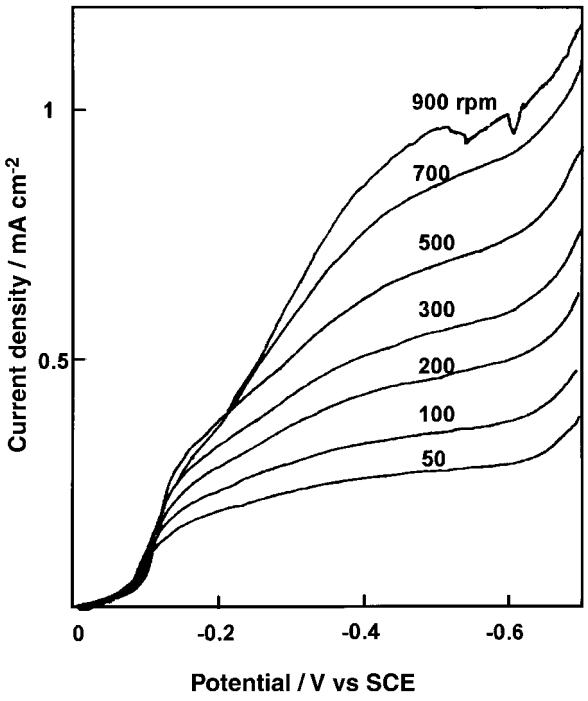

Fig. 1. Variation of current with potential for different rotation speeds. [Cu(II)] = 50 ppm. $dE/dt = 0.001$ V s^{-1}.

3.2. *Cobalt electrodeposition*

Cobalt deposition from sulphate solutions was analysed in a similar way. The variation of the current–potential curves with rotation speed is shown in Figure 2. The voltammograms show a limiting current zone in the potential range from −1.3 to −1.8 V, showing a displacement toward more cathodic values with increasing rotation speed. The limiting current values are much higher than those obtained with copper. Since hydrogen evolution occurs simultaneously with metal reduction, this effect may be due to the movement of gas bubbles, which increases the convective mass transport rate. Other authors have also observed a limiting current, although under different conditions [35–37]. In chloride media this is related to mass transport control [37], but in sulphate media it may be associated to an adsorption limited process, since it is sensitive to the presence of organic additives [35].

3.3. *Minimum electrodeposition potentials*

In order to establish the minimum potential at which electrodeposition of Co and Cu could be achieved onto vitreous carbon, linear sweep measurements were carried out at a low sweep rate of 0.1 mV s^{-1}. Minimum electrodeposition potentials were determined by extrap-

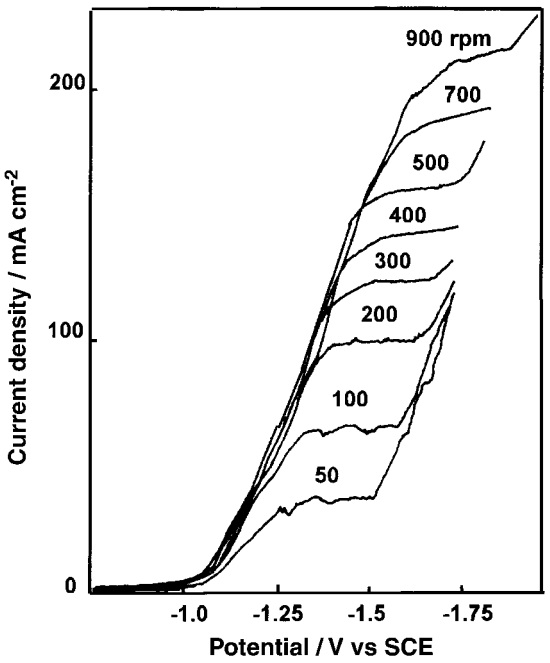

Fig. 2. Variation of the current with the potential for different rotation speeds. [Co(II)] = 100 ppm. $dE/dt = 0.001$ V s^{-1}.

olation of the slope of the rising curve to the base line, in the zone where the current starts to increase [2]. Results for cobalt with different solution concentrations are shown in Figure 3 as an example.

The values found for both metals are summarised in Table 1 and the theoretical equilibrium potentials, E_e, of the respective reactions are also indicated. As expected, copper electrodeposition exhibits low overpotential. On the other hand, cobalt deposition on vitreous carbon proceeds with an overpotential of 400 mV. Hydrogen evolution is the competitive secondary reaction, which depends strongly on electrode material. In 0.5 M Na_2SO_4, pH 2, it begins at -1.2 V on vitreous carbon, at -0.75 V on copper and at -0.95 V on cobalt. Consequently changes in cobalt deposition must be expected when there are copper ions in solution.

3.4. *Electrodeposition from mixed cation solutions*

A basic electrochemical analysis was performed of the influence of the metal ion concentrations on cobalt and copper deposition on a vitreous carbon substrate. The

Table 1. Equilibrium potentials and minimum deposition potentials for copper and cobalt

Concentration /ppm	Cu^{2+}/Cu		Co^{2+}/Co	
	E_e/V*	$E_{dep,min}$/V*	E_e/V*	$E_{dep,min}$/V*
500	0.043	−0.025	−0.578	−0.925
100	0.013	−0.05	−0.599	−0.995
50	0.004	−0.095	−0.609	−1.012

*All potentials are with respect to SCE

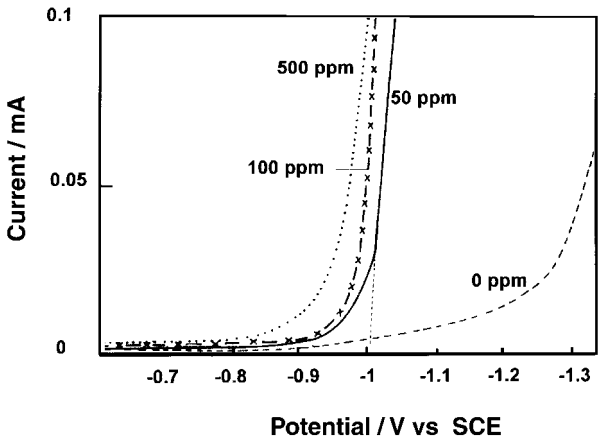

Fig. 3. Minimum potential of cobalt deposition. $dE/dt = 0.1$ mV s^{-1}, $\omega = 500$ rpm.

behaviour of binary mixtures of Cu–Co was investigated by linear sweep voltammetry.

In Figure 4, starting at 0 V in the cathodic direction, the first distinctive feature is the limiting current due to copper deposition, although it is scarcely visible due to the current scale. At -0.8 V, the current increases due to the simultaneous reactions of hydrogen evolution and cobalt electrodeposition. When copper concentrations are of order 500 ppm, the limiting current corresponding to Co codeposited with copper is not observed. In the anodic direction, two peaks are observed at -0.4 V and 0.35 V, which correspond to cobalt and copper dissolution respectively.

Figure 5 shows the anodic zone of continuous voltammograms obtained with different concentrations of Co(II) and Cu(II). Peak A corresponds to copper dissolution. This appears at 0.1 V at low concentrations and there is a shift in the peak potential in the positive direction for more concentrated solutions while the peak size increases considerably. The presence of Co(II) does not modify this behaviour significantly. Peak B arises from cobalt dissolution and reaches a maximum at -0.35 V when pure metal is deposited. Under these conditions a small peak near 0 V also appears whose origin is currently under study.

When both metals are deposited simultaneously, the cobalt behaviour changes. If [Cu(II)] = 50 ppm, peak B disappears and a third peak (C) appears at intermediate potentials between A and B. With increasing copper concentration, this new peak shifts towards more positive values (-0.15 V) until it merges with peak A and at the same time peak B reappears at -0.45 V.

Both peaks B and C can be attributed to cobalt oxidation, which was incorporated into the electrodeposit structure under different conditions. Peak B is associated with the oxidation of bulk cobalt. This reaction is affected by the presence of a greater quantity of copper in solution, which produces either a change in reaction mechanism or a modification of surface morphology. Peak C may be due to the preferential

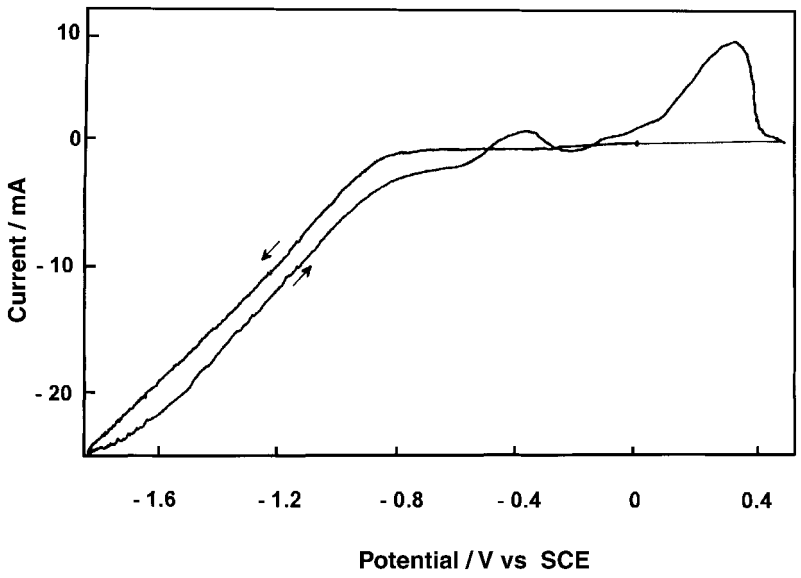

Fig. 4. Continuous sweep voltammogram showing cobalt and copper deposition and dissolution. [Cu(II)] = [Co(II)] = 500 ppm, dE/dt = 0.01 V s^{-1}, ω = 500 rpm.

dissolution of Co either from a Cu–Co alloy or dispersed among copper crystallites or covered by the more noble metal in the course of the anodic sweep. In the latter case, oxidation becomes difficult because cobalt must dissolve through the copper network.

On the other hand, the possible formation of a Cu/Co alloy can not be discarded. This alloy would dissolve at more positive potential than the less noble metal, thus giving rise to peak C. Even though the Cu/Co phase diagram shows that this system has practically no solubility of either copper in cobalt or cobalt in copper at room temperatures [39], oversaturated solid solutions have been obtained over a wide concentration range using mechanical alloying [19] and molecular beam epitaxy [23]. Furthermore, it has been found for other systems, such as Cu–Pb [13], that even though the solid

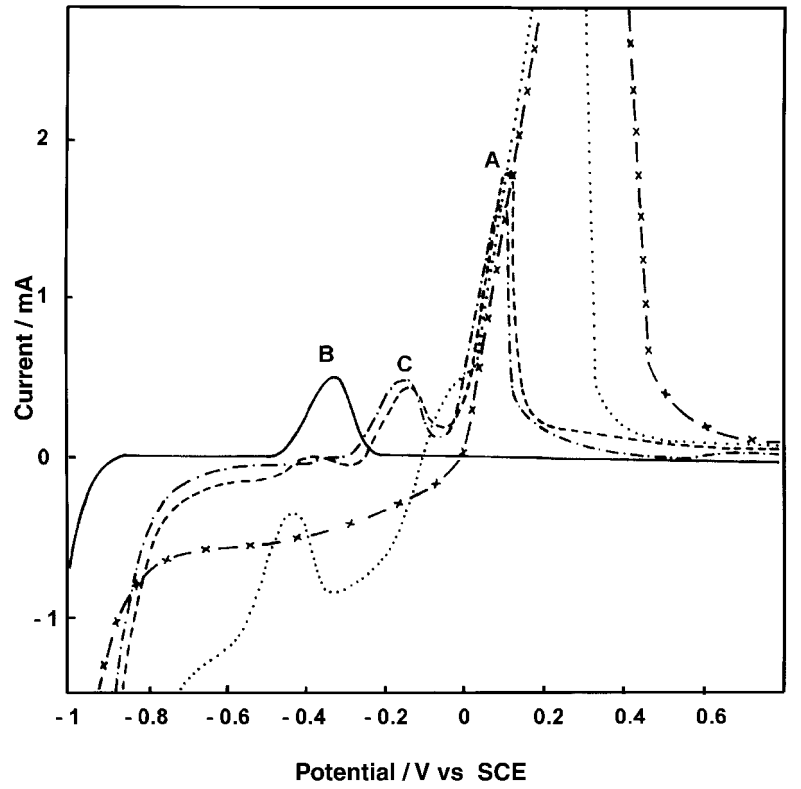

Fig. 5. Effect of the concentration in the anodic zone of the continuous linear sweep voltammograms. Electrolyte composition: (——) [Co(II)] = 500 ppm, (– · –) [Co(II)] = 500 ppm, [Cu(II)] = 50 ppm, (– – –) [Co(II)] = 500 ppm, [Cu(II)] = 100 ppm, (· · ·) [Co(II)] = 500 ppm, [Cu(II)] = 500 ppm, (×——×) [Cu(II)] = 500 ppm. dE/dt = 0.01 V s^{-1}, ω = 500 rpm, E_c = −1.4 V, E_a = +0.8 V.

lead solubility in copper is very small in alloys obtained by metallurgical processes, the lead content is in the order of 10 wt.% in electrodeposited alloys. In the electrodeposition of multilayer thin films, it seems that Co–Cu films form a solid solution over a wide range of composition [26].

Anodic linear sweep voltammetry (ALSV) [4] has proved to be a useful tool for the characterisation of binary alloys. In this work, it was used to obtain more information about the behaviour of the binary system when greater amounts of metals were deposited under potentiostatic conditions. Therefore, the electrode potential was maintained at −1.4 V for 5 min to form the deposits and then anodic dissolution was carried out using a slow sweep in the positive direction.

The i/E curves for different relationships of concentrations of the metallic ions are shown in Figure 6. Two peaks are observed (A and B) which correspond to the dissolution of bulk metals, copper and cobalt, respectively, as well as a shoulder (D) at more positive potentials. Peak B appears at −0.08 V in the absence of Cu(II). When small quantities of Cu(II) are added, no significant modifications are observed except that a shoulder appears at 0.1 V corresponding to the dissolution of the more noble metal. When the [Cu(II)] to [Co(II)] ratio is 1:1, peak B shifts to more cathodic potentials, while a well-defined peak A can be seen at 0.18 V. Shoulder D does not vary in height, but is displaced to more positive potentials with increasing copper concentration.

It is evident that peaks B and D correspond to cobalt oxidation because they are not observed when the solution contains only copper ions, but no evidence of alloy formation is found under these conditions. Both cobalt peaks can be attributed to dissolution of zones of the electrodeposit with different metal distribution or phase structure. A similar explanation has been offered for zinc and cobalt codeposition [17, 39, 40]. Therefore, codeposition of both metals modifies cobalt dissolution behaviour, but it does not influence the copper response. To clarify the nature of the dissolution peaks, X-ray diffraction studies will be carried out to characterize the crystalline structure before dissolution.

3.5. *EDAX analysis of deposits obtained at constant potentials*

EDAX microanalysis results from different binary mixtures are shown in Table 2. The samples were prepared maintaining the rotating disk electrode at a constant potential for 5 min. The mapping of the samples indicates that both metals are uniformly distributed on all surfaces. With respect to the metal atomic concentration, deposits appear richer in copper than may be expected from the solution concentrations. Even at −1.4 V, cobalt is deposited in smaller proportion because cobalt deposition is probably being carried out at currents lower than the limiting current density. Test 6 shows that copper could be recovered without great interference of cobalt until potentials in the order of −1.0 V.

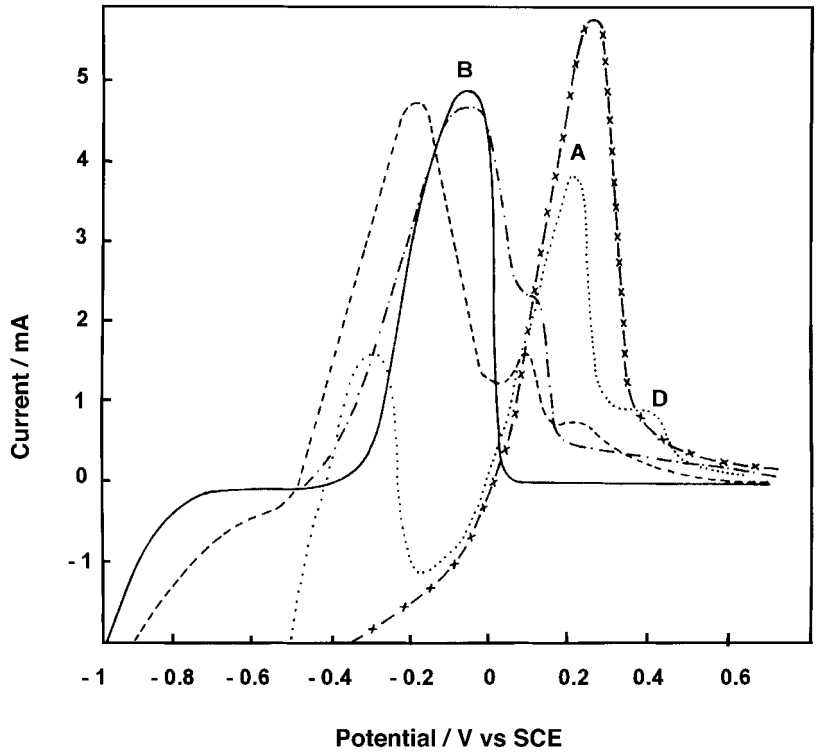

Fig. 6. Anodic linear sweep voltammograms, obtained after maintaining the electrode at −1.4 V for 5 min. Electrolyte composition: (——) [Co(II)] = 500 ppm, (– · –) [Co(II)] = 500 ppm, [Cu(II)] = 50 ppm, (– – –) [Co(II)] = 500 ppm, [Cu(II)] = 100 ppm, (· · ·) [Co(II)] = 500 ppm, [Cu(II)] = 500 ppm, (×——×) [Cu(II)] = 500 ppm. dE/dt = 0.01 V s^{-1}, ω = 500 rpm.

Table 2. EDAX analysis of electrodeposit obtained at constant potential onto a vitreous carbon rotating disc electrode ($\omega = 500$ rpm)

Sample	E_{dep} /V vs SCE	[Cu(II)] /ppm	[Co(II)] /ppm	Cu /at. %	Co /at. %
1	−1.4	50	500	11.2	88.8
2	−1.4	500	50	98.4	1.6
3	−1.4	50	50	61.9	38.1
4	−1.4	500	500	64.3	35.7
5	−1.2	500	500	89.5	10.5
6	−1.0	500	500	98.1	1.9

Figure 7 shows SEM micrographs of two samples corresponding to different concentration ratios. The morphology of the deposits varies according to the copper concentration in solution. When the cobalt concentration is highest the deposits are more compact (Figure 7(a)). With increasing copper content, they become more porous with abundant production of dendrites (Figure 7(b)).

This variation explains the changes in cobalt behaviour shown in Figure 6. When copper concentration decreases, cobalt must be dissolved from compact crystals with a smaller surface area where cobalt probably forms a more homogeneous mixture with copper. With increasing copper concentration the structure appears more open and rough, with the likelihood that some of the codeposited cobalt is more exposed to the dissolution, while the rest is coated with copper and will only dissolve when the noblest metal is oxidized.

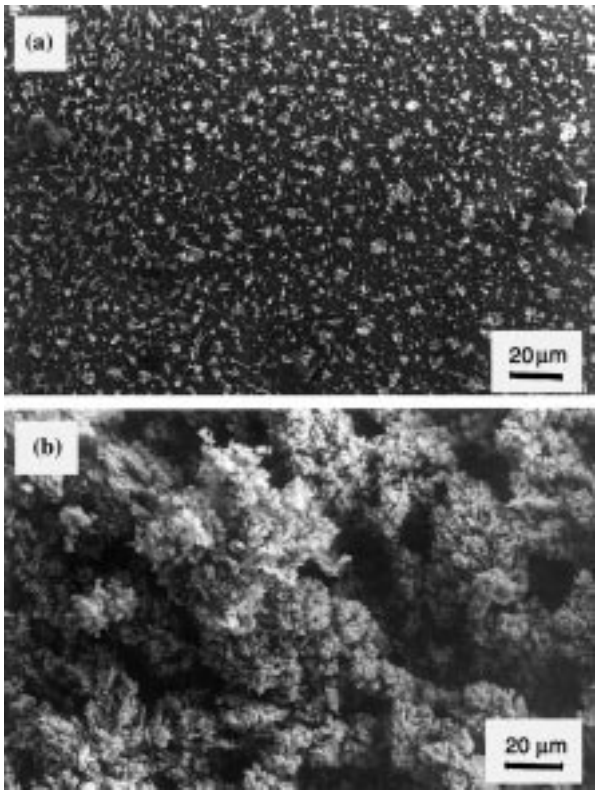

Fig. 7. SEM micrographs from deposits obtained after maintaining the electrode at −1.4 V for 5 min. (a) [Cu(II)] = 50 ppm, [Co(II)] = 500 ppm, ×480; (b) [Cu(II)] = 500 ppm, [Co(II)] = 500 ppm, ×480.

3.6. *Copper and cobalt recovery current efficiency tests*

According to the above mentioned results, copper deposition is the prevailing process when attempting to recover copper and cobalt from a solution containing both ions in low concentration. To verify whether the same conclusions were applicable to greater scale conditions, tests were made using a laboratory batch reactor with a RVC rotating cylinder cathode.

Both ions were electrodeposited at constant potential for 4 h, measuring the variation of current with time to calculate the total coulombic charge. The partial charges for each electrodeposited species were determined from concentration changes of metal ions in solution. Current efficiencies (η) and conversions (χ) [41] were calculated as

$$\eta = \frac{zFV(C_0 - C_f)}{Q_t} \times 100$$

$$\chi = \frac{C_0 - C_f}{C_0} \times 100$$

where V is the reactor volume, C_0 is the initial concentration, C_f is the final concentration, and Q_t is the total charge.

The mass transfer coefficient, k_m, was calculated from the copper concentration decay, using the following equation:

$$\frac{C(t)}{C_0} = \exp\left(-\frac{k_m A}{V}t\right)$$

Assuming a specific surface area of 50 cm^{-1} a value of $k_m = 1.4 \times 10^{-3}\,cm\,s^{-1}$ was calculated, which is comparable with results obtained by other authors using RVC rotating cylinders although of different porosity [42].

Cobalt deposition was difficult under the conditions of the experiments. Conversion was below 10% in all tests. This result was unexpected since cobalt deposition had been detected previously in tests effected on a small rotating disc electrode under similar conditions. The cause is probably a strong increase of the ohmic drop due to the electrode resistance and higher current densities.

Current efficiency and conversion for copper after 4 h electrolysis are shown in Table 3. From these results, it can be seen that copper efficiency decreases as concentration of the ion in solution decreases and the deposition potential shifts in the negative direction. On the other hand, conversion increases when the initial copper concentration is reduced. However, this trend changes if cobalt is added to the solution, as can be seen from the results for more negative potentials. Since there is no unique tendency, the influence of cobalt on copper

Table 3. Effect of potential and [Cu(II)] to [Co(II)] ratio on efficiency and conversion for copper recovery

Potential vs SCE Concentration /ppm	−0.6 V		−1.0 V		−1.4 V	
	η /%	χ /%	η /%	χ /%	η /%	χ /%
10 Cu	24.9	55.5	20	60.8	–	–
50 Cu	64.4	40.2	38.3	76.5	–	–
100 Cu	71	13.5	75.8	22	–	–
10 Cu + 500 Co	14.5	27	20.8	61.8	13.4	61.6
50 Cu + 500 Co	42	48.2	43.6	66.7	30	83
100 Cu + 500 Co	82.2	26.9	59.3	87.9	53.6	92.2

electrodeposition is not clear. This, therefore, will be the subject of further studies.

4. Conclusions

(i) EDAX tests indicate that copper can be deposited without cobalt interference at potentials as cathodic as −1.0 V despite high Co concentrations.

(ii) At a more negative potential, both metals are deposited simultaneously though the copper proportion in the binary mixture is greater than that corresponding to the solution concentration ratio, indicating that probably cobalt is not deposited at limiting current conditions. This effect is also detectable when the [Co(II)]/[Cu(II)] ratio is very high, in the order of 10 to 1.

(iii) Voltammetry studies effected under conditions in which codeposition occurs show only minor changes in copper behaviour. On the other hand, cobalt behaviour exhibits significant modifications. Even though formation of an intermetallic compound is possible, ASVL and microscopy tests indicate cobalt deposition in different crystalline forms as the more probable cause. In turn, cobalt deposition depends on the polarization conditions of the electrode and on cobalt and copper concentrations. This last factor probably determines the morphology and porosity of the Co/Cu deposit which, in turns, determines the existence of compact zones, in which cobalt must dissolve through a net of copper crystallites.

(iv) The morphology of the deposits varies according to the [Co(II)]/[Cu(II)] ratio. When cobalt prevails, deposits are more compact. With increasing copper content they become more porous with abundant formation of dendrites.

Acknowledgements

The authors acknowledge the financial support of the Universidad Nacional del Sur and the Comisión de Investigaciones Científicas de la Provincia de Buenos Aires.

References

1. D. Pletcher and F.C. Walsh, 'Industrial Electrochemistry' (Chapman & Hall, 1990).
2. R.D. Armstrong, M. Todd, J.W. Atkinson and K. Scott, *J. Appl. Electrochem.* **26** (1996) 379.
3. J.A. Trainham and J. Newman, *J. Electrochem. Soc.* **124** (1977) 1528.
4. D.N. Bennion and J. Newmn, *J. Appl. Electrochem.* **2** (1972) 113.
5. K. Scott, *J. Appl. Electrochem.* **18** (1988) 504.
6. F. Coeuret, *J. Appl. Electrochem.* **10** (1980) 687.
7. R.P. Tison, *J. Electrochem. Soc.* **128** (1981) 317.
8. D. Pletcher and F.C. Walsh, *in* D. Genders and N. Weinberg (Eds), 'Electrochemistry for a Cleaner Environment' (The Electrosynthesis Company, 1992), New York.
9. F.C. Walsh, *in* D. Genders and N. Weinberg (Eds), 'Electrochemistry for a Cleaner Environment' (The Electrosynthesis Company, 1992), New York.
10. M. Schwartz, R. Suzuki and K. Nobe, *in* E.W. Brooman and J.M. Fenton (Eds), 'Electrochemical Technology Applied to Environmental Problems', Proceedings of the Electrochemical Society **95–12** (1995), p. 81.
11. K. Scott and W.K. Lui, *in* 'Electrochemical Engineering', The Institution of Chemical Engineers, Symposium Series No. 98, (1986), p. 161.
12. A.J. Chaudhary and S.M. Grimes, *J. Chem. Tech. Biotechnol.* **56** (1993) 15.
13. V.D. Jović, R.M. Zejnilović, A.R. Despić and J.S. Stevanović, *J. Appl. Electrochem.* **18** (1988) 511.
14. A.R. Despić, *in* O.J. Murphy (Ed.), 'Electrochemistry in Transition' (Plenum Press, New York, 1992), p. 453.
15. V.D. Jović, A.R. Despić, J.S. Stevanović and S. Spajić, *Electrochim. Acta* **34** (1989) 1093.
16. J.S. Stevanović, A.R. Despić and V.D. Jović, *Electrochim. Acta* **42** (1997) 873.
17. E. Gómez and E. Vallés, *J. Electroanal. Chem.* **421** (1997) 157.
18. V.D. Jović, N. Tošicc and M. Stojanović, *J. Electroanal. Chem.* **420** (1997) 43.
19. V.M. López-Hirata and E.M. Arce-Estrada, *Electrochim. Acta* **42** (1997) 61.
20. Y. Jyoko, S. Kashiwabara and Y. Hayashi, *J. Electrochem. Soc.* **144** (1997) L5.
21. M. Alper, K. Attenborough, R. Hart, S.J. Lane, D.S. Lashmore, C. Younes and W. Schwarzacher, *Appl. Phys. Lett.* **63** (1993) 2144.
22. G.L. Zhou and C.P. Flynn, *Phil. Mag. Lett.* **76** (1997) 315.
23. G.L. Zhou, M.H. Yang and C.P. Flynn, *Phys. Rev. Lett.* **77** (1996) 4580.
24. A. Blondel, B. Doudin and J.P. Ansermet, *J. Magnetism and Magnetic Mater.* **165** (1997) 34.
25. Y. Jyoko, S. Kashiwabara and Y. Hayashi, *J. Electrochem. Soc.* **144** (1997) L193.
26. H. Zaman, A. Yamada, H. Fukuda and Y. Ueda, *J. Electrochem. Soc.* **145** (1998) 565.

27. M. Dariel, L.H. Bennett, D.S. Lashmore, P. Lubitz, M. Rubinstein, W.L. Lechter and M.Z. Harford, *J. Appl. Phys.* **61** (1987) 4067.
28. K.D. Bird and M. Schlesinger, *J. Electrochem. Soc.* **142** (1995) L65.
29. Hach Company, 'Handbook for Analysis of Surface Finishing Solutions' (1987).
30. V.Yu. Filinovsky and Yu.V. Pieskov, *in* E. Yeager, J. O'Bockris, B.E. Conway and S. Sarangapani. (Eds), 'Comprehensive Treatise of Electrochemistry', Vol. 9, (Plenum Press, New York, 1984).
31. T.I. Quickenden and Q. Xu, *J. Electrochem. Soc.* **143** (1996) 1249.
32. S. Kariuki and H.D. Dewald, *Electroanalysis* **8** (1996) 307.
33. L. Gertz and F. Lapicque, *J. Electrochem. Soc.* **143** (1996) 3910.
34. D. Pletcher, I. Whyte, F.C. Walsh and J.P. Millington, *J. Appl. Electrochem.* **21** (1991) 659.
35. T.C. Franklin and A. Aktan, *J. Electrochem. Soc.* **135** (1988) 1636.
36. M.C. Vilchenski, A.V. Benedetti and P.T.A. Sumodjo, Joint International Meeting, Paris 1997, The Electrochemical Society and The International Society of Electrochemistry, Meeting Abstract, p. 1894.
37. C.Q. Cui, S.P. Jiang and A.C.C. Tseung, *J. Electrochem. Soc.* **137** (1990) 3418.
38. H. Baker (Ed.), 'ASM Handbook', Vol. 3, 'Alloy Phase Diagrams' Materials Park, Ohio (1992).
39. C. Karwas and T. Hepel, *J. Electrochem. Soc.* **136** (1989) 1672.
40. I. Kirilova, I. Ivanov and St. Rashkov, *J. Appl. Electrochim.* **27** (1997) 1380.
41. F.C. Walsh, 'A First Course in Electrochemical Engineering' (The Electrochemical Consultancy, ROMSEY, England, 1993).
42. A.H. Nahlé, G.W. Reade and F.C. Walsh, *J. Appl. Electrochem.* **25** (1995) 450.